HERA Event Generators for the Low Mass Region

Victor Lendermann

DESY, Notkestr. 85, 22607 Hamburg, Germany

1 Introduction

As an ep collider with centre-of-mass energy of about 300 GeV HERA provides us with detailed and extensive knowledge about high energy photo-hadronic interactions. The hadronic final state in the studied reactions has typically high invariant mass and high particle multiplicity. For the simulation of such interactions and the generation of the hadronic final state a two-step scheme is commonly used. First, QCD hard subprocesses are generated and higher orders are approximated by an appropriate parton shower model. Subsequently, the fragmentation is performed usually employing the Lund string generator PYTHIA [1] or alternatively the HERWIG generator [2].

However there are a number of exclusive and semi-inclusive reactions measured at HERA, in which the hadronic final state has a low mass, of the order of one to several GeV. Such processes usually involve low virtualities of the exchanged photon, Q^2, which restricts the applicability of pQCD, and thus requires special models for the interaction. Furthermore the standard Lund string fragmentation cannot be applied without additional tuning at masses below 5 GeV. Hence the usual event generation scheme has to be modified or alternative procedures have to be employed. Several such dedicated models utilised in HERA data analyses are discussed in this article.

The availability of reliable Monte Carlo models for the domain in question opens the possibility for new precision measurements. The most ambitious goal is the measurement of the proton structure function F_2, extending the HERA kinematic range towards the region previously covered only by fixed target experiments and beyond.

In the next section typical processes involving low mass hadronisation are briefly presented. A special emphasis is put on the possibility of measuring the proton structure function F_2 in the extended kinematic domain. Afterwards three models for the simulation of hadronic final state in this region are described.

2 Processes Involving Low Mass Hadronisation

One of the extensively studied fields at HERA involving low mass hadronisation is diffraction. A common theoretical treatment of the diffractive

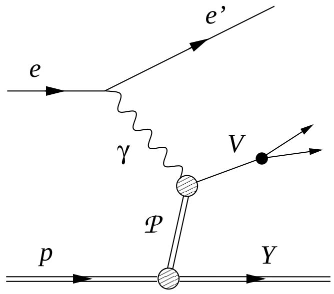

Fig. 1. Vector meson production in Regge model

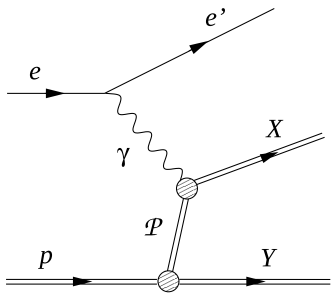

Fig. 2. Inclusive diffraction in Regge model

processes is based on the Regge approach, which assumes an exchange of a colour-neutral object, pomeron or reggeon, between the proton and the photon. The pomeron exchange results in a large rapidity gap between the hadronic final state measured in the detector and the proton remnant.

An example of such processes is diffractive photo- and electroproduction of vector mesons. The corresponding Feynman diagram in the Regge model is depicted in fig. 1. In these reactons the proton either stays intact or dissociates into a mostly low mass hadronic final state. For MC simulations the event generators DIFFVM [3] and EPSOFT [4–6] are often employed in the H1 [7] and ZEUS [8] analyses, respectively. For the dissociative case, these generators contain dedicated models of low mass hadronisation at the proton–pomeron vertex. In the HERA analyses the separation of elastic and inelastic contributions is accomplished by detecting signals in the forward detector components. However the acceptance limits do now allow the complete separation at low masses and the acceptance corrections have to be estimated from the simulation.

A similar process is Deeply Virtual Compton Scattering (DVCS), in which, instead of a vector meson, a photon is detected in the final state. DVCS has attracted special attention in the last years, since it allows in particular an extraction of skewed parton distributions. So far there are calculations of the elastic channel only, and the first HERA measurement results for the elastic scattering were recently published [9]. More precise measurements of this process, which are foreseen in the HERA II program, shall demand a more precise estimation of the hadronisation corrections and hence a detailed simulation of the hadronic final state.

Simulation of low mass hadronisation is also required in the analyses of inclusive diffraction (fig. 2). In the H1 measurements [10] of the diffractive DIS cross section, diffractive structure function $F_2^{D(3)}$, diffractive jet production etc. the presence of the rapidity gap is ensured by demanding that no dissociation occurs at the proton–pomeron vertex. Similar criteria are also applied in the ZEUS analyses [11]. As in the studies of vector meson production, for

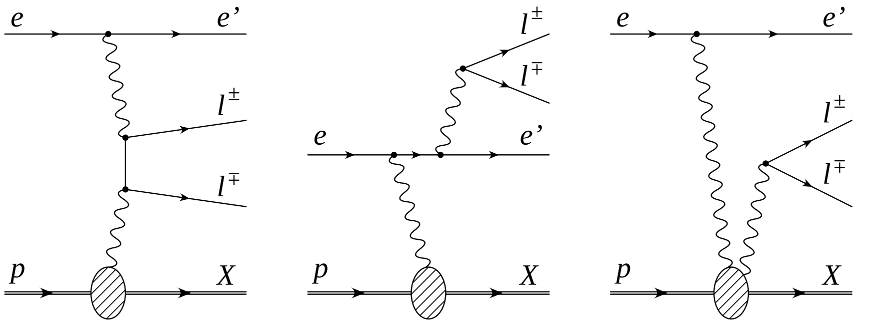

Fig. 3. Leading order Feynman diagrams for lepton pair production

the estimation of the acceptance correction the DIFFVM or EPSOFT models are employed. The obtained correction is typically of the order of 5 – 10 % and even bigger, depending on the event selection.

An example of a non-diffractive reaction involving low hadronic masses is continuum dilepton production, described by the Feynman diagrams in fig. 3. This process constitutes one of the dominant background sources for J/ψ production and for searches for new physics at HERA. For simulations the event generator GRAPE [12] is presently employed. It provides a very precise cross section calculation including all diagrams of the electroweak theory. The event generation is completed by the simulation of the hadronic final state, which is performed by the SOPHIA package [13].

Finally, QED Compton scattering (QEDC) is another process, for which a good simulation of low mass hadronisation is of special importance. QEDC corresponds to one of the peaks in the ep cross section with a photon radiation from the lepton side, as described by the Feynman diagrams in fig. 4. In QEDC events the outgoing electron and photon are observed at relatively large polar angles in the main detector almost back-to-back in azimuth, so that their total transverse momentum is close to zero. This allows access to the domain of very low Q^2, and opens the possibility to measure the proton structure function F_2 in the transition region from DIS to photoproduction.

The experimental selection of the QEDC signal restricts the kinematic region to relatively high values of the Bjorken x variable or equivalently low masses of the hadronic final state. The reason for such a selection is a high contribution of the inclusive DIS background at low x, in which the final state photon is faked by a particle from the hadronic final state (mostly π^0). The x–Q^2 distribution of generated QEDC events after applying realistic cuts is displayed in fig. 5.

For this simulation the generator COMPTON [14] was employed. The actual version of the generator [15] includes all three hadronisation packages mentioned above, DIFFVM, EPSOFT and SOPHIA, thus allowing the direct comparison of the models to each other and to the HERA data. The simula-

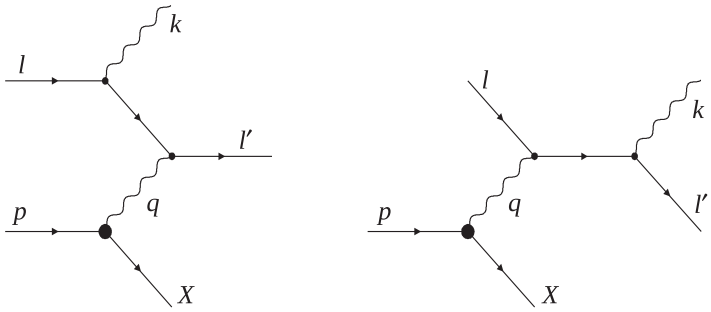

Fig. 4. Leading order Feynman diagrams for *ep* scattering with photon emission from the lepton line

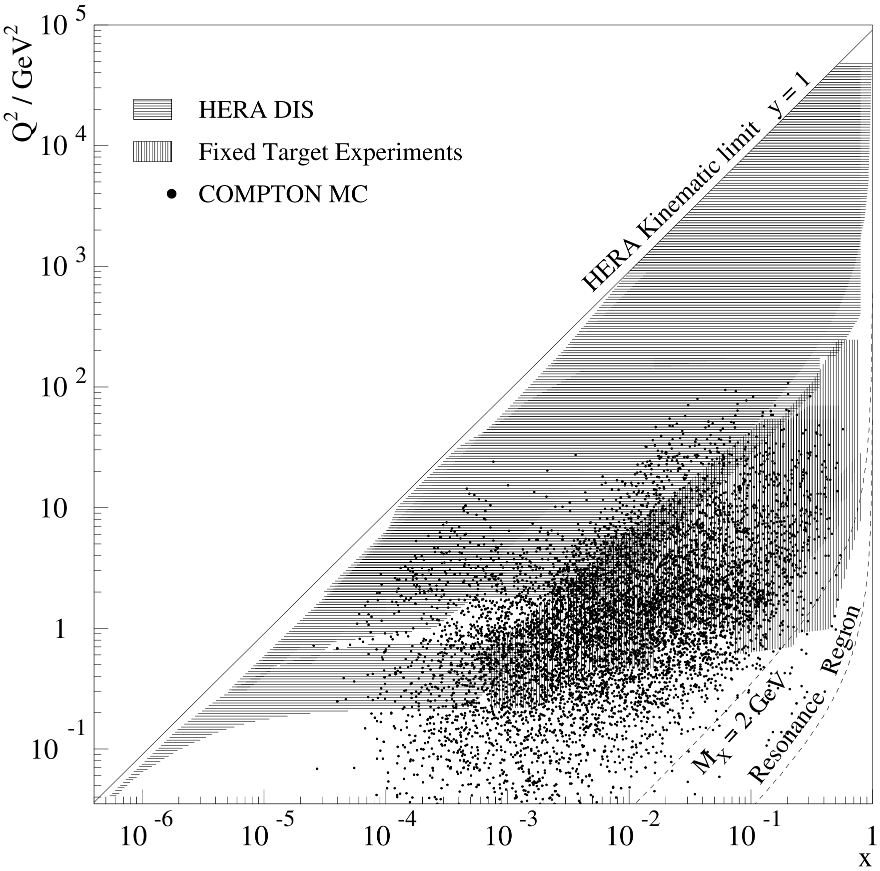

Fig. 5. Kinematic domain of inelastic QED Compton scattering for a typical event selection in contrast to the regions of inclusive DIS measurements at HERA and fixed target experiments

tion of the hadronic final state is necessary not only for the description of the detector acceptance corrections but also for the reconstruction of the Bjorken x variable, since in this kinematic region the method utilising the parameters of the outgoing electron and photon provides very poor x resolution.

In the following section an overview of the hadronisation models is given.

3 Hadronisation Models

3.1 DIFFVM

The hadronisation procedure implemented in the DIFFVM generator [3] includes production of nuclear resonances, and two different options for simulation in the continuum region. The first one is a simplistic approach, in which the proton is split into a quark and a diquark, and the pomeron is assumed to transfer the momentum to the quark. Afterwards a Lund string is stretched between the quark and the diquark and the subsequent fragmentation is performed by PYTHIA/JETSET.

This method involves both problems mentioned in the introduction and therefore the program includes another model, in which hadrons are produced directly, and the final state consists of one proton or neutron and a number of pions. Assuming isospin symmetry, twice as many charged pions are generated on average as neutral pions.

The charged particle multiplicity is given according to KNO scaling [16]. This term denotes the fact, experimentally observed in diffractive high energy hadron collisions [17], that the average number of charged particles depends only on the invariant hadronic mass M and the actual multiplicities in events are spread normally around this value. The mean multiplicity, $N_\pm$, and the width of the Gaussian distribution, $\sigma_\pm$, are calculated according to [18] as

$$\begin{aligned} N_\pm &= 2N_c \; , \\ \sigma_\pm &= N_\pm/2 \; , \end{aligned} \qquad N_c = \begin{cases} \sqrt{M_r} & \text{for } M_r \le 1 \; , \\ a_1 \ln^2 M_r + b_1 \ln M_r + c_1 & \text{for } M_r > 1 \; , \end{cases} \tag{1}$$

with parameters: $a_1 = 0.36$, $b_1 = 0.13$, $c_1 = 1$. Here, N_c is the mean multiplicity of charged pairs, and the residual mass variable M_r is given by

$$M_r = \frac{M - m_p}{1\,\mathrm{GeV}} \; , \tag{2}$$

where m_p is the proton mass. The above parameterisation was obtained in [18] by fitting data from CERN experiments performed at the pp colliders ISR with centre-of-mass energy $\sqrt{s} = 60\,\mathrm{GeV}$ and SPS with $\sqrt{s} = 540\,\mathrm{GeV}$.

After the final state particles have been defined, an isotropic phase space decay of the hadronic mass M into these particles is executed by the package RAMBO *(Random Momentum Booster)* [19]. A well known problem of the phase space decay is that in the case of large masses and a low number of pions it produces particles with too large transverse momenta at variance with experimental observations.

3.2 EPSOFT

The fragmentation of a low hadronic mass in EPSOFT [4,5] is an optimised procedure of the HERWIG soft underlying event hadronisation [2], which, in turn, is based on the minimum bias event generator of the UA5 collaboration [20]. The parameters were tuned to reproduce hadron–hadron and ZEUS photoproduction data.

In the first step of fragmentation the charged pair multiplicity n_c is chosen. In the standard version of the generator it is spread according to the negative binomial distribution (NBD):

$$P(n_c) = \frac{{N_c}^{n_c} k^k}{(N_c + k)^{n_c+k}} \frac{\Gamma(n_c + k)}{n_c!\,\Gamma(k)} \tag{3}$$

with $1/k = 0.05$ around the mean value:

$$N_c = a_2 \ln^2 M_r + b_2 \ln M_r + c_2 \tag{4}$$

with $a_2 = 0.176$, $b_2 = 0.43132$ and $c_2 = 0.86224$. The total number of charged particles is $2n_c + 1$. At $M_r < 1$, n_c is set to zero, meaning that there is only one charged particle in the final state. As can be seen in fig. 6, the parameterisation (4) yields much lower multiplicities at high masses than (1) indicating that there may be a discrepancy between the SPS pp and the ZEUS γp data.

In a ZEUS study [6], focused at very low masses $M < 5\,\mathrm{GeV}$, the negative binomial distribution in EPSOFT was replaced by a Gaussian, since the NBD was found to fail for hadron–hadron data in this region. This version thus employs almost the same multiplicity model as used by DIFFVM. The optimal procedure may be to split the mass range into two parts and use a Gaussian distribution for low masses and NBD for high masses. In this way the EPSOFT model is implemented into the COMPTON generator.

In the second step the particle content of the hadronic state is defined. The flavours of the valence quarks of final state hadrons are selected according to the scheme depicted in fig. 7 that automatically conserves charge, isospin and strangeness. In this algorithm adding a new hadron involves extending the quark flavour chain by one element that can be a light quark (u, d or s) or a diquark line. The flavours are picked randomly with probabilities adjusted so as to produce hadrons in ratios close to those measured in hadron–hadron interactions [21]. If the valence quark flavours do not define the hadron uniquely, the one with the smallest mass is chosen. The procedure is repeated until $2n_c + 1$ charged hadrons are obtained.

After the hadron content is specified, the transverse momenta of particles are generated according to the probability distribution

$$\frac{\mathrm{d}P}{\mathrm{d}p_t^2} \propto \exp\left(-\kappa\sqrt{p_t^2 + m^2}\right) \tag{5}$$

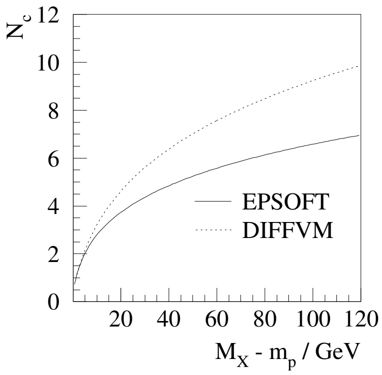

Fig. 6. Average multiplicity of charged particle pairs as a function of the residual mass of the hadronic final state

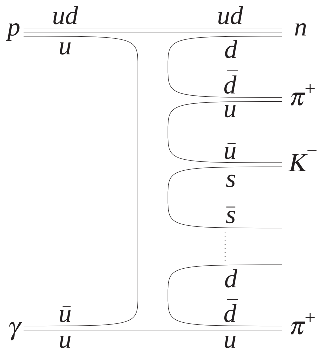

Fig. 7. Final state hadron generation through valence quark flow in EPSOFT

where the slope parameter κ is computed as:

$$\kappa = \frac{d}{a \ln^2 M_r + b \ln M_r + c} \tag{6}$$

with $a = 0.00175$, $b = 0.00167$, $c = 0.353$ and $d = 2$. For strange particles κ is reduced by factor 0.6.

In the last step the generation of the longitudinal momenta is performed from the flat rapidity distribution with Gaussian shoulders based on the technique described in [22].

3.3 SOPHIA

The recently developed generator SOPHIA *(Simulations of Photohadronic Interactions in Astrophysics)* [13] provides a minimum bias description of photoproduction processes reproducing a large set of available data. To be specific, the production of major nuclear resonances, direct pion production and multiparticle generation including the diffractive production of light vector mesons are implemented. The choice of a particular process at a given mass M is made by sampling from the corresponding cross section fits, depicted in fig. 8. Decays of unstable particles are performed by the routine DECSIB from the SIBYLL package [23].

Non-diffractive multiparticle production, which is the dominant contribution within the acceptance of HERA detectors, is based on the Dual Parton Model [24]. This approach was previously implemented for the simulation of soft photohadronic interactions in the PHOJET generator [25], which has been successfully applied for the description of photoproduction at HERA. In this model the incoming proton and photon are split into coloured quark and diquark constituents, which exchange their quantum numbers in the course

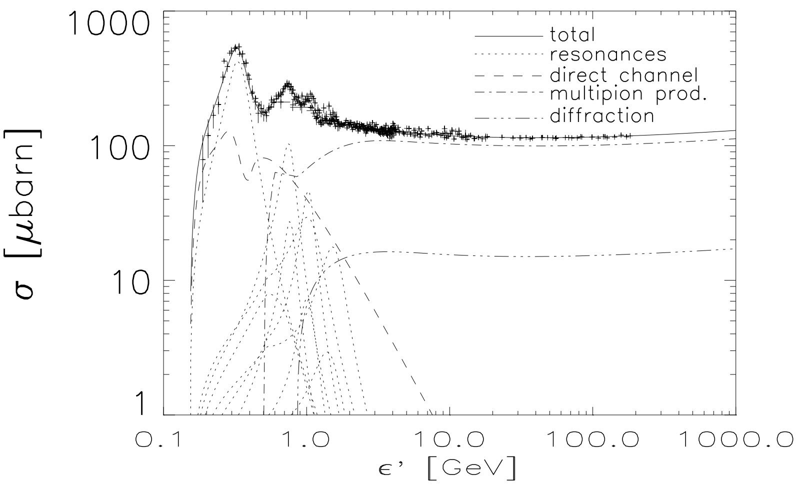

Fig. 8. Total γp cross section (*solid line*) as implemented in SOPHIA with the contributions of baryon resonances (*dotted line*), direct pion production (*dashed line*), non-diffractive multiparticle production (*dash-dotted line*), and diffractive vector meson production (*dash-triple-dotted line*) plotted as functions of the photon energy in the proton rest frame. Figure from [13]

of interaction. The arising colour field forces result into the colour strings which subsequently fragment to hadrons.

The parton configurations are related to pomeron and reggeon exchange in this model. The pomeron exchange corresponds to the formation of two strings, while in case of the reggeon exchange one string is stretched between the diquark in the proton and the quark in the photon (see fig. 9). The pomeron and reggeon contributions are calculated according to [26] as:

$$\sigma_{\mathrm{reg}} \propto \left(\frac{M^2 - m_p^2}{s_0}\right)^{-0.34} \qquad \sigma_{\mathrm{pom}} \propto \left(\frac{M^2 - m_p^2}{s_0}\right)^{0.095} \tag{7}$$

with the reference scale $s_0 = 1\,\mathrm{GeV}^2$.

The quark and diquark flavours inside the proton are determined by the spin and valence flavour statistics. For photons the ratio of probabilities to couple to an $u\bar{u}$ or a $d\bar{d}$ pair is assumed to be 4:1 due to the charge difference between u and d quarks.

The longitudinal momentum fractions of partons connected to the string are based on Regge asymptotics [27] One obtains for the valence quark (x) and diquark ($1-x$) momentum distributions inside the proton:

$$\rho(x) \sim \frac{1}{\sqrt{x}}(1-x)^{\frac{3}{2}} \ , \tag{8}$$

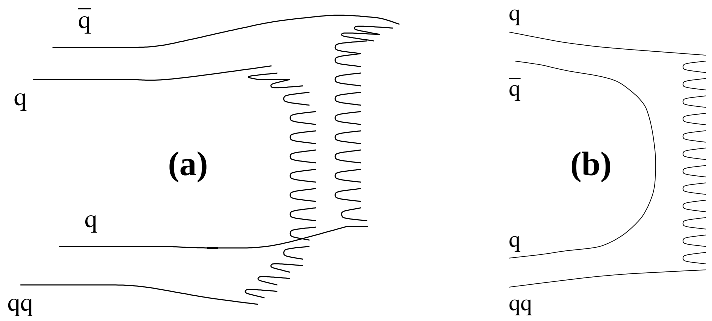

Fig. 9. String formation in the Dual Parton Model in the case of **(a)** pomeron and **(b)** reggeon exchange. Figures from [13]

and for the quark and antiquark distributions inside the photon:

$$\rho(x) \sim \frac{1}{\sqrt{x(1-x)}} \ . \tag{9}$$

The transverse momenta of the partons at the string ends are neglected.

The string fragmentation is done by the PYTHIA/JETSET routines. Several parameters of the fragmentation code have been tuned in order to obtain a reasonable description at small hadronic masses.

4 Summary

A number of processes are measured at HERA at low invariant masses of the hadronic final state. Several dedicated models are available for the simulations in this domain. These models open new possibilities for precision measurements, in particular, for an extention of the kinematic region of F_2 measurements.

References

1. T. Sjöstrand et al.: Comput. Phys. Commun. **135**, 238 (2001)
2. G. Corcella et al.: JHEP **0101**, 010 (2001)
3. B. List: Diploma Thesis, Technical University of Berlin (1993)
4. M. Kasprzak: Doctoral Thesis, University of Warsaw (1996)
5. M. Inuzuka: private communication
6. L. Adamszyk: Doctoral Thesis, University of Krakow (1999)
7. C. Adloff et al. [H1 Collaboration]: Eur. Phys. J. C **10**, 373 (1999)
   C. Adloff et al. [H1 Collaboration]: Eur. Phys. J. C **13**, 371 (2000)
   C. Adloff et al. [H1 Collaboration]: Phys. Lett. B **483**, 23 (2000)
   C. Adloff et al. [H1 Collaboration]: Phys. Lett. B **483**, 360 (2000)
   C. Adloff et al. [H1 Collaboration]: Phys. Lett. B **520**, 191 (2001)

C. Adloff et al. [H1 Collaboration]: Phys. Lett. B **539**, 25 (2002)
C. Adloff et al. [H1 Collaboration]: Eur. Phys. J. C **25**, 25 (2002)
C. Adloff et al. [H1 Collaboration]: Eur. Phys. J. C **25**, 41 (2002)
C. Adloff et al. [H1 Collaboration]: Phys. Lett. B **541**, 251 (2002)

8. M. Derrick et al. [ZEUS Collaboration]: Phys. Lett. B **380**, 220 (1996)
M. Derrick et al. [ZEUS Collaboration]: Z. Phys. C **73**, 73 (1996)
J. Breitweg et al. [ZEUS Collaboration]: Z. Phys. C **75**,215 (1997)
J. Breitweg et al. [ZEUS Collaboration]: Eur. Phys. J. C **2**, 247 (1998)
J. Breitweg et al. [ZEUS Collaboration]: Phys. Lett. B **437**, 432 (1998)
J. Breitweg et al. [ZEUS Collaboration]: Eur. Phys. J. C **6**, 603 (1999)
J. Breitweg et al. [ZEUS Collaboration]: Eur. Phys. J. C **14**, 213 (2000)
J. Breitweg et al. [ZEUS Collaboration]: Phys. Lett. B **487**, 273 (2000)
9. C. Adloff et al. [H1 Collaboration]: Phys. Lett. B **517**, 47 (2001)
10. C. Adloff et al. [H1 Collaboration]: Z. Phys. C **76**, 613 (1997)
C. Adloff et al. [H1 Collaboration]: Eur. Phys. J. C **6**, 421 (1999)
C. Adloff et al. [H1 Collaboration]: Eur. Phys. J. C **20**, 29 (2001)
11. J. Breitweg et al. [ZEUS Collaboration]: Eur. Phys. J. C **1**, 81 (1998)
J. Breitweg et al. [ZEUS Collaboration]: Eur. Phys. J. C **6**, 43 (1999)
12. T. Abe: Comput. Phys. Commun. **136**, 126 (2001)
13. A. Mücke, R. Engel, J. P. Rachen, R. J. Protheroe and T. Stanev: Comput. Phys. Commun. **124**, 290 (2000)
14. T. Carli, A. Courau, S. Kermiche and P. Kessler: in **Proceedings of the Workshop “Physics at HERA”, Hamburg, 1991**, DESY, 1992, Vol. 2, pp. 902–915 and Vol. 3, pp. 1468–1472
15. V. Lendermann: Doctoral Thesis, University of Dortmund (2001)
16. Z. Koba, H. B. Nielsen and P. Olesen: Nucl. Phys. B **40**, 317 (1972)
17. R. L. Cool, K. Goulianos, S. L. Segler, H. Sticker and S. N. White: Phys. Rev. Lett. **48**, 1451 (1982)
18. K. Goulianos: Phys. Rept. **101**, 169 (1983)
19. R. Kleiss, W. J. Stirling and S. D. Ellis: Comput. Phys. Commun. **40**, 359 (1986)
20. G. J. Alner et al. [UA5 Collaboration]: Nucl. Phys. B **291**, 445 (1987)
21. G. Marchesini and B. R. Webber: Nucl. Phys. B **310**, 461 (1988)
22. S. Jadach: Comput. Phys. Commun. **9**, 297 (1975)
23. R. S. Fletcher, T. K. Gaisser, P. Lipari and T. Stanev: Phys. Rev. D **50**, 5710 (1994)
24. A. Capella, U. Sukhatme, C. Tan and J. Tran Thanh Van: Phys. Rept. **236**, 225 (1994)
25. R. Engel: Z. Phys. C **66**, 203 (1995)
R. Engel and J. Ranft: Phys. Rev. D **54**, 4244 (1996)
26. A. Donnachie and P. V. Landshoff: Phys. Lett. B **296**, 227 (1992)
27. A. Capella, U. Sukhatme and J. Tran Thanh Van: Z. Phys. C **3**, 329 (1979)
A. Capella and J. Tran Thanh Van: Z. Phys. C **10**, 249 (1981)
A. B. Kaidalov: Phys. Lett. B **116**, 459 (1982)
A. B. Kaidalov and K. A. Ter-Martirosian: Phys. Lett. B **117**, 247 (1982)